Carbon 114 (2017) 217–223

Contents lists available at ScienceDirect

Carbon

journal homepage: www.elsevier.com/locate/carbon

Nanoenergetic material-on-multiwalled carbon nanotubes paper chip as compact and flexible igniter

Kyung Ju Kim [a, 1], Hun Jung [a, 1], Ji Hoon Kim [a], Nam Soo Jang [a], Jong Man Kim [a, b], Soo Hyung Kim [a, b, *]

[a] Department of Nano Fusion Technology, College of Nanoscience and Nanotechnology, Pusan National University, 30 Jangjeon-dong, Geumjung-gu, Busan 609-735, Republic of Korea
[b] Department of Nano Energy Engineering, College of Nanoscience and Nanotechnology, Pusan National University, 30 Jangjeon-dong, Geumjung-gu, Busan 609-735, Republic of Korea

ARTICLE INFO

Article history:
Received 24 September 2016
Received in revised form
5 December 2016
Accepted 7 December 2016
Available online 9 December 2016

ABSTRACT

A compact and flexible multiwalled carbon nanotubes (MWCNTs)-coated paper electrode was fabricated in this study. The shape of the paper electrode could be varied simply by cutting it. Further, its electrical resistance did not change appreciably either when it was bent with different curvatures or when it was subjected to repeated bending and stretching. An nanoscale energetic material (nEM)-on-MWCNTs paper chip formed by depositing an nEM thin film on the MWCNTs-coated paper electrode could be stably ignited by applying voltages higher than ~ 15 V. The ignition and explosion characteristics of the chip were investigated systematically. It was found that the explosion reactivity of the chip increased with an increase in the thickness of the nEM thin film. Finally, the remote ignition of the nEM-on-MWCNTs paper chip was successfully demonstrated by explosively breaching a door, suggesting that such nEM-on-MWCNTs paper chips can be used as compact, flexible, and versatile igniters in various civil and military applications.

1. Introduction

Carbon nanotubes (CNTs) are often called the jewel of nanotechnology owing to their unique properties, employed from traditional mechanical, electrical and material engineering fields to newly emerging energy, environmental and biomedical technologies [1–8]. The high rates of electron and heat transfer of CNTs are among their most useful characteristics, making them attractive for use in a wide range of applications. It is known that these properties are strongly affected by a number of parameters, including whether the CNTs undergo transformations as well as by their structure and the impurities present in them [9–23].

Nanoscale energetic materials (nEMs) consist of nanoscale fuel and oxidizer materials, which contain chemical energy and can rapidly release it in the form of pressure and thermal energy when ignited by an external energy input [24–29]. Aluminum (Al) is mainly used as a fuel material, while various metal oxides such as NiO, TiO_2, WO_3, MoO_3, Fe_2O_3, $KMnO_4$ are used as an oxidizer. The combustion and explosion reactivity of nEMs are strongly affected by various characteristics, including the size, morphology and chemical composition and degree of intermixing between fuel and oxidizer. When nEMs are ignited by external energy input, a so-called self-sustaining exothermic reaction occurs. These nEMs with strong exothermic characteristics can be applied in various thermal engineering fields such as explosives, propellants, and pyrotechnics.

In order to ignite nEMs, a number of traditional methods exist such as mechanical impact or those involving the use of a flame or electric spark. Even though these traditional methods of igniting nEMs are very effective, they have a few inherent limitations with respect to their use in the field of thermal engineering, which can involve relatively large, complex, and rigid mechanical parts and

* Corresponding author. Department of Nano Fusion Technology, College of Nanoscience and Nanotechnology, Pusan National University, 30 Jangjeon-dong, Geumjung-gu, Busan 609-735, Republic of Korea.
E-mail address: sookim@pusan.ac.kr (S.H. Kim).
[1] Both K. J. Kim and H. Jung equally contributed to this work as the first authors.

http://dx.doi.org/10.1016/j.carbon.2016.12.021
0008-6223/

electric circuits. Therefore, inexpensive, compact, and flexible heaters are often required for developing small thermal igniters for both civil and military applications such as rocket motors, airbags, and fire extinguishers [30–33].

When an electrode is made of pure metal-based thin films (e.g., Al, Cu, etc.), its electrical resistance can be easily increased due to the formation of an oxide film [34–36]. In addition, the metal thin films can be easily broken when it is bent, and thus the deposition of metal thin films on flexible substrates is not easy to realize. Unlike these metal thin films, CNTs have the advantages of reduction in oxidation problems and relatively easy formation of flexible thin films. Multiwalled carbon nanotubes (MWCNTs), which are potential electrode materials, are used widely in various electrical and thermal engineering fields [37–43]. In this study, we aimed to develop compact, flexible, and versatile igniters, in which a thin film of nEM is fabricated on the surface of a MWCNTs-coated paper electrode (hereafter labeled as an nEM-on-MWCNTs paper chip). The nEM-on-MWCNTs paper chip is consisted of a compact, inexpensive, and flexible conductive paper electrode, and it is a simple, easy-to-use, and portable igniter and allowed for remote ignition and controlled explosion when combined with appropriately designed electrical circuits.

The compact, flexible, and versatile igniter composed of an nEM-on-MWCNTs paper chip was designed and manufactured by coating an nEMs layer on the surface of a regular MWCNTs-coated paper electrode. Specifically, Al nanoparticles (Al NPs) as fuel and copper oxide nanoparticles (CuO NPs) as oxidizer were used as the nEMs components. Regular MWCNT-coated paper was employed as the heat generation and transfer medium as well as a flexible substrate. The ignition, combustion, and explosion characteristics of the nEM-on-MWCNTs paper chip were examined systematically by using different applied voltages and nEMs-based thin films of different thicknesses. Finally, the remote ignition of the nEM-on-MWCNTs paper chip was demonstrated successfully by combining it with a wireless electric signal processing system, with the aim of demonstrating its suitability for the remote explosive breaching of doors.

2. Experimental

MWCNTs (CNT Co. Ltd, Korea) manufactured by the thermal and chemical vapor deposition method were employed in this study. The MWCNTs, which were used without further purification, had a purity of ~95%, an average diameter of ~20 nm, length distribution of 1–25 μm, and specific surface area of ~250 m^2/g.

Fig. 1a shows a schematic of the first step, which was a MWCNT thin film coated on the surface of a piece of regular nonconductive paper by using the vacuum filtration method. In brief, the MWCNTs (0.3 wt%) were dispersed in an ethanol solution and then ultrasonicated at 750 W and 20 kHz for 30 min. A circular piece of regular paper with a diameter of 4.5 cm was placed on a filter supporter in a suction flask, and a vacuum was formed using a vacuum pump in the lower part of the flask. Next, ~3 ml of the MWCNT solution was poured slowly into the vacuum filtering equipment by using a micropipette. This resulted in the MWCNTs being filtered on the paper, with the ethanol solution passing through the paper and into the flask below. The MWCNT-thin-film-coated paper was then dried at room temperature for 30 min and cut into electrodes of the desired sizes and shapes. The electrical resistance of MWCNT-thin-film-coated papers formed by various experimental conditions was measured as shown in Fig. S1 in supporting information. Electric lines and clips were connected to the MWCNTs-coated paper electrode for applying various voltages, which varied the temperature of the fabricated electrode.

In the second step, a simple spin-coating process was employed to form an nEM thin film on the fabricated MWCNTs-coated paper electrode, as depicted in Fig. 1b. Specifically, nEMs consisting of Al NPs (NT base, Korea) with an average diameter of ~80 nm (used as the fuel metal) and CuO NPs (NT base, Korea) with an average diameter of ~100 nm (used as the oxidizer) was employed in this

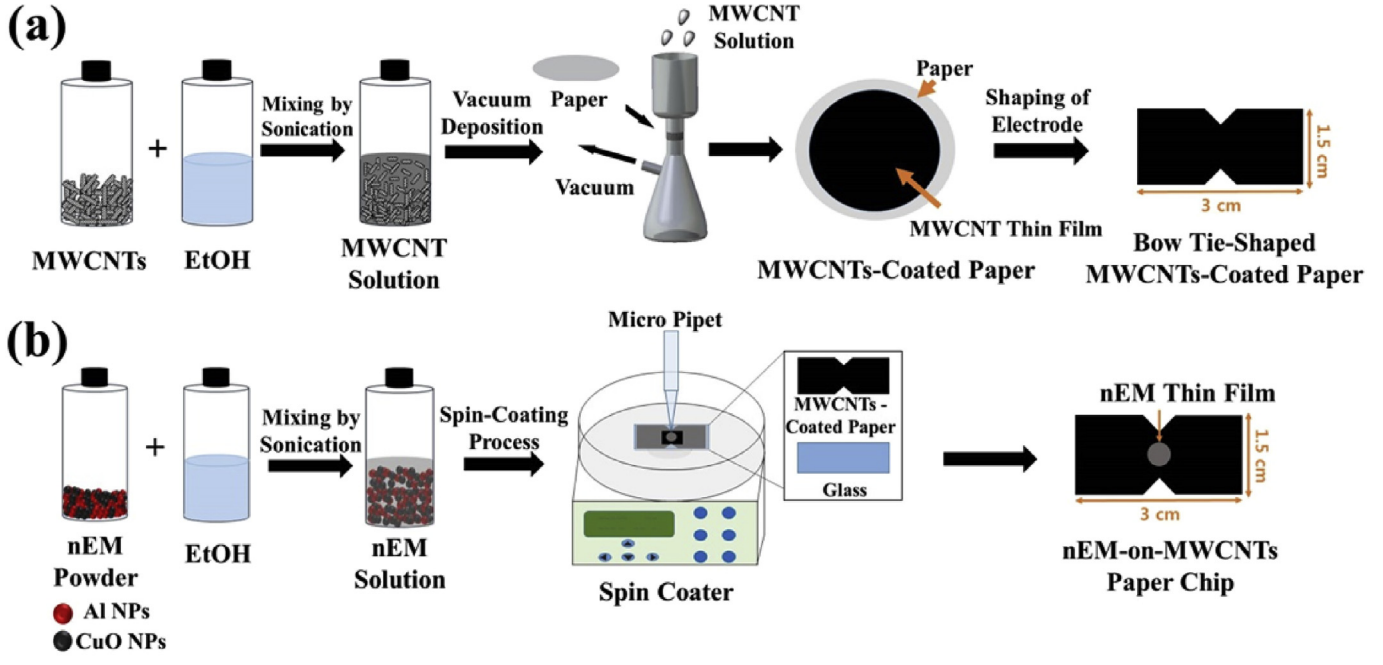

Fig. 1. Schematics showing the fabrication of (a) the MWCNT solution, the MWCNTs-coated paper formed using the vacuum filtration method, and the bow-tie-shaped MWCNTs-coated paper electrode. Schematics showing the fabrication of (b) the nEM solution by mixing Al and CuO NPs in an ethanol solution and the nEM thin film on the MWCNTs-coated paper electrode formed using the spin-coating process. Photographs of the nEM-on-MWCNTs paper chip fabricated in this study. (A colour version of this figure can be viewed online.)

study. The nEM powder was fabricated by mixing the Al NPs and CuO NPs (Al/CuO = 30:70 wt%) for 30 min using ultrasonication energy (Ultrasonic power input = 170 W, frequency = 40 kHz) in an ethanol solution. Next, ~10 μl of the nEM solution was drop cast on the MWCNTs-coated paper electrode by using a micropipette (3–25 μl), and the electrode was rotated using a spin coater at 300 rpm for 30 s to form an nEM thin film.

In the final step, different voltages were applied to the nEM-on-MWCNTs paper chip to test its ignition and explosion characteristics, which were monitored using a high-speed camera (Photron, FASTCAM SA3 120K) at a frame speed of 30 kHz. The high-speed camera used in this study had a maximum frame rate of 1,200,000 fps, sensor size of 17.4 mm × 17.4 mm (CMOS image sensor), and pixel size of 17 μm × 17 μm. The electrical resistance measurements and ignition tests of nEM-on-MWCNTs paper chip were performed under normally RH 50% condition.

3. Results and discussion

Fig. 2a shows an image of a bow-tie-shaped MWCNT-coated paper electrode having a length of 3 cm, width of 1.5 cm, and neck width of 0.7 cm fabricated in this study. It also shows top- and side-view scanning electron microscopy (SEM) images of the bow-tie-shaped MWCNT-coated paper electrode. It was observed that the MWCNTs were homogeneously cross-linked, with the thickness of the MWCNT thin film being ~80 μm, which was very close to that of the paper substrate. In addition, the MWCNT thin film was strongly attached to the paper substrate. This was confirmed by 3M tape peel-off and water washing tests as shown in Fig. S2 in supporting information.

To examine the effects of the bending of the MWCNT-coated paper electrode on its electrical resistance, the paper electrode was manually wrapped on the surfaces of plastic tubes with

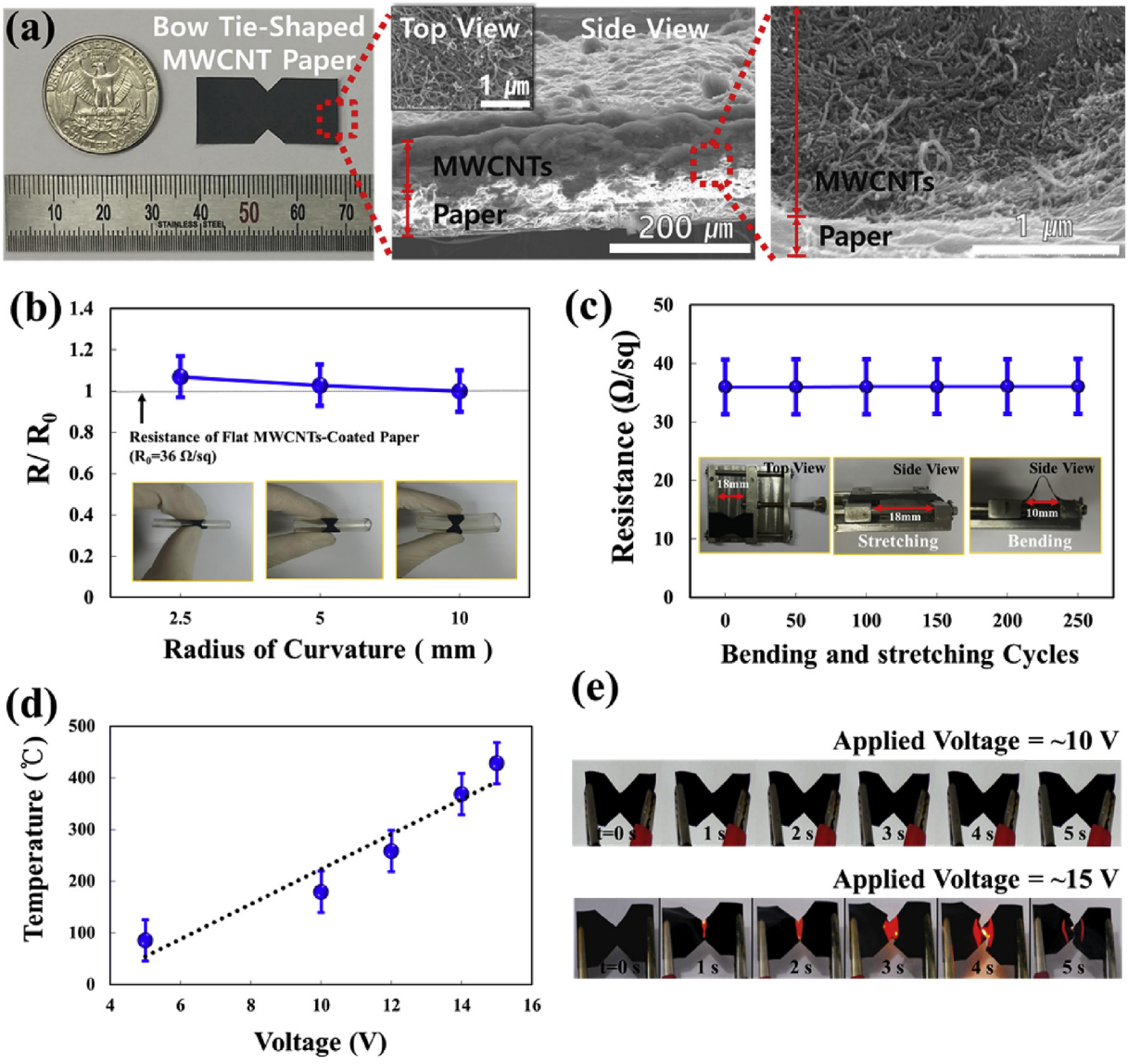

Fig. 2. (a) Photograph of the fabricated bow-tie-shaped MWCNT-coated paper electrode, side-view SEM image showing the MWCNT thin film coated on the paper substrate (Inset is a high-resolution SEM image of the top view of the MWCNT thin film), and high-resolution side-view SEM image showing the boundary layer between the MWCNT thin film and the paper substrate. (b) Changes in the electrical resistance of the paper electrode with the radius of curvature and (c) electrical resistance of the paper electrode as a function of the number of bending-and-stretching cycles (Insets are images of the paper electrode during repeated bending and stretching at a radius of curvature of 2.5 mm). (d) Changes in the temperature of the paper electrode as a function of the applied voltage and (e) snapshots of the paper electrode under applied voltages of ~10 and ~15 V. (A colour version of this figure can be viewed online.)

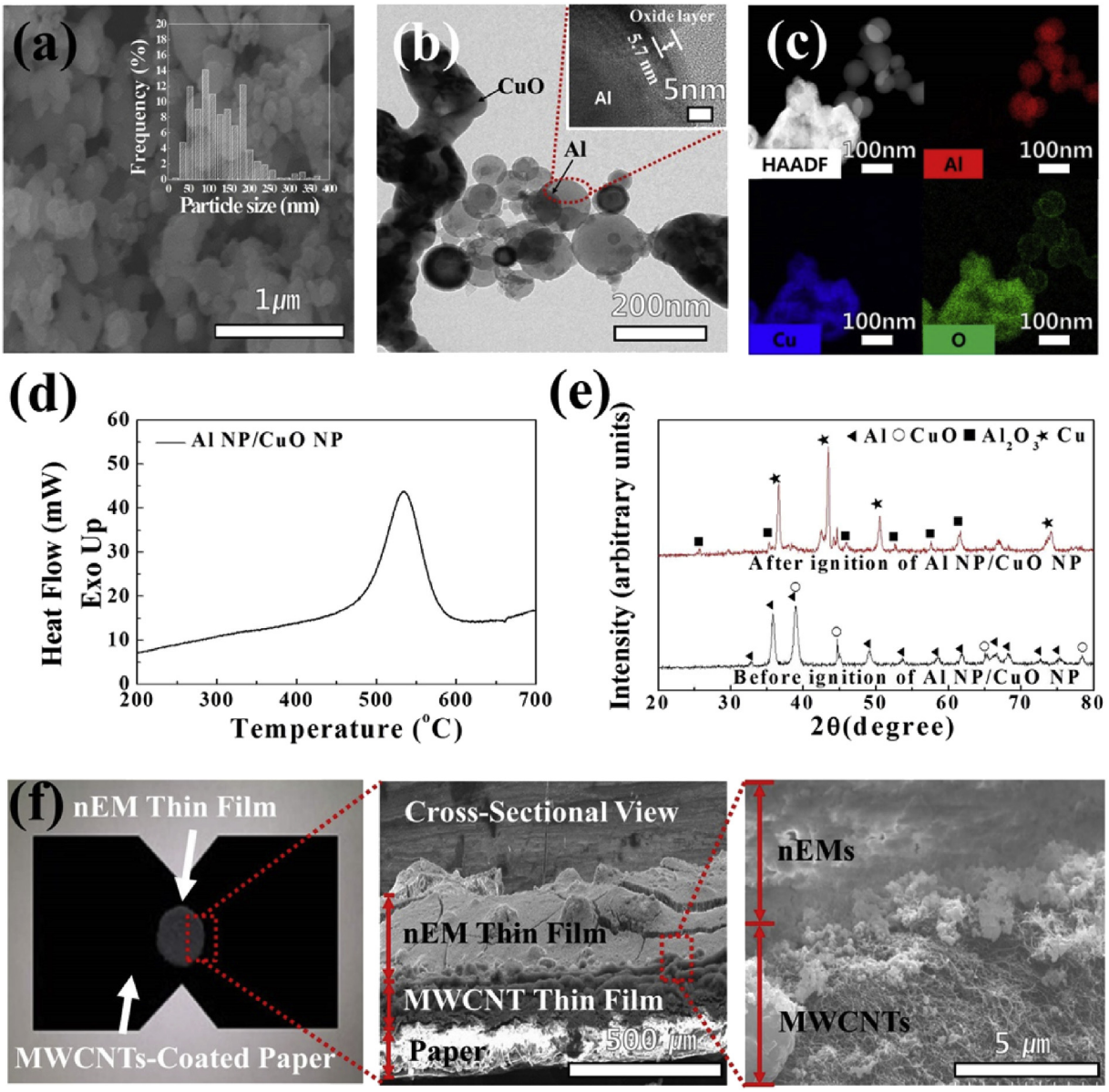

Fig. 3. (a) SEM image (inset shows the particle size distribution), (b) TEM image (inset shows a high-resolution TEM image of the Al NPs with an oxide layer with a thickness of ~6 nm), (c) STEM image and elemental maps, and (d) DSC curve of the Al/CuO nanocomposite. (e) XRD spectra of the Al/CuO nanocomposite before and after ignition, and (f) photograph and SEM image (cross-sectional view) of the spin-coated nEM thin film formed on the MWCNTs-coated paper electrode (the magnified images are high-resolution SEM images of the boundary layer between the nEM thin film and the MWCNTs-coated paper electrode). (A colour version of this figure can be viewed online.)

different curvatures, and the electrical resistance was measured 20 times at each experimental condition. The average value and error range of resistance were presented after removing the highest and lowest values, as shown in Fig. 2b. The electrical resistances for the different radii of curvature were found to be R/R_0 = ~1.07 @R2.5 mm, R/R_0 = ~1.02 @R5 mm, and R/R_0 = ~1.00 @R10 mm, indicating that the electrical resistance increased slightly with a decrease in the radius of curvature. This was presumably because microscale cracks formed in the MWCNT thin film, resulting in tensile and compressive stresses on the top and bottom surfaces, respectively, of the film. The resulting relaxation of the MWCNTs and the microcracks formed caused a decrease in the electrical mobility of the electrons, retarding their movement.

To examine the effects of the repeated bending of the MWCNT-coated paper electrode on its electrical resistance, a series of bending and stretching tests was performed, as shown in Fig. 2c. The electrical resistance of the MWCNT-coated paper electrode did not change appreciably even after being subjected to bending and stretching for up to ~250 cycles, suggesting that not only did the MWCNT thin film remain strongly attached to the paper substrate but the MWCNTs also remained tightly bonded to each and readily returned to their original structure once the bending force was released.

To investigate the suitability of the fabricated MWCNT-coated paper electrode as a heater, different voltages were applied to the paper electrode. The temperature at the center of the narrow neck area of the bow-tie-shaped electrode was measured using an optical pyrometer (Testo 845, Testo AG. Co.), as shown in Fig. 2d. It was observed that the temperature increased linearly with the applied voltage. It is interesting to note that the electrode ignited and burned at an applied voltage of ~15 V; this corresponded to a temperature of ~430 °C, which is very close to the ignition

temperature of regular paper (400–450 °C). Fig. 2e shows that the neck area of the bow-tie-shaped electrode did not ignite at an applied voltage of ~10 V. However, when the voltage was increased to ~15 V, it ignited within 1 s. The flame started to spread from the neck to the electrode and was suddenly extinguished owing to a short circuit caused by the electrode separating completely into two parts within 3–4 s. This suggested that the fabricated MWCNT-coated paper electrode can be used as an ignition platform that ignites when the appropriate voltage is applied.

Fig. 3a and b show SEM and TEM images of the used nEMs, which were composed of Al NPs and CuO NPs. It can be seen that, in the Al NPs/CuO NPs-based nEM powder, both the spherical Al NPs and the agglomerated CuO NPs were closely connected to each other. The average particle diameter of the Al/CuO nanocomposite was approximately 90 ± 5 nm, and the thickness of the aluminum oxide layer on the Al NPs was approximately 6 nm, as shown in Fig. 3b and c. Fig. 3d shows the results of the differential scanning calorimetry (DSC) measurements performed to evaluate the total reaction heat energy generated by the nEMs. A distinct peak corresponding to an exothermic reaction was observed at temperatures of 450–600 °C. The integration of the exothermic curve yielded the total heat of the exothermic reaction, which was approximately 1361 J/g. Fig. 3e shows the X-ray diffraction (XRD) patterns of the Al/CuO nanocomposite before and after the ignition test. The presence of both Al and CuO was confirmed before ignition. However, after the flame-induced ignition and combustion of the Al/CuO nanocomposite, the peaks related to Al and CuO disappeared, while strong peaks related to Cu and Al_2O_3 appeared. This suggested that the nEM underwent a phase change owing to the ignition and combustion processes, as per the following redox reaction: $2Al + 3CuO \rightarrow Al_2O_3 + 3Cu$. Fig. 3f shows a photograph and an SEM image (cross-sectional view) of the spin-coated nEM thin film formed on the previously fabricated bow-tie-shaped MWCNT-coated paper electrode. The nEM thin film was composed of Al NPs and CuO NPs, as can be seen from the scanning TEM (STEM) images in Fig. 3c. Further, the thin film had a diameter of ~5 mm and a thickness of ~150 μm, and it was formed in the center of neck of the bow-tie-shaped MWCNTs-coated paper electrode. The images also showed that the nEM thin film and the MWCNTs-coated paper electrode were in good contact with each other.

The ignition and explosion characteristics of the nEM-on-

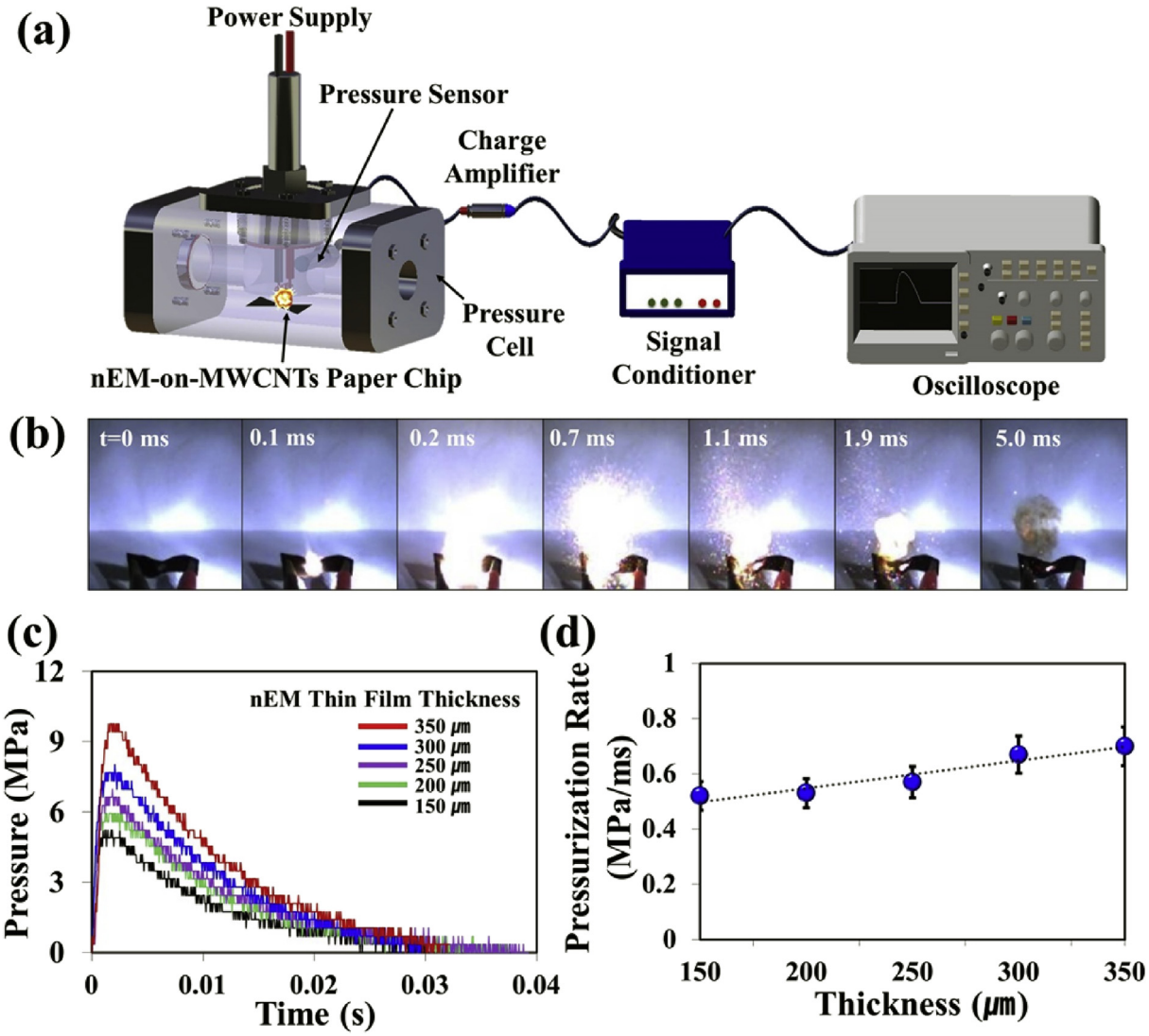

Fig. 4. (a) Schematic of the confined pressure cell tester used, (b) snapshots showing the ignition and subsequent explosion of the nEM-on-MWCNTs paper chip (the thickness of the nEM thin film was ~150 μm), and (c) pressure traces and (d) pressurization rates of nEM-on-MWCNTs paper chips with nEM thin films of various thicknesses. (A colour version of this figure can be viewed online.)

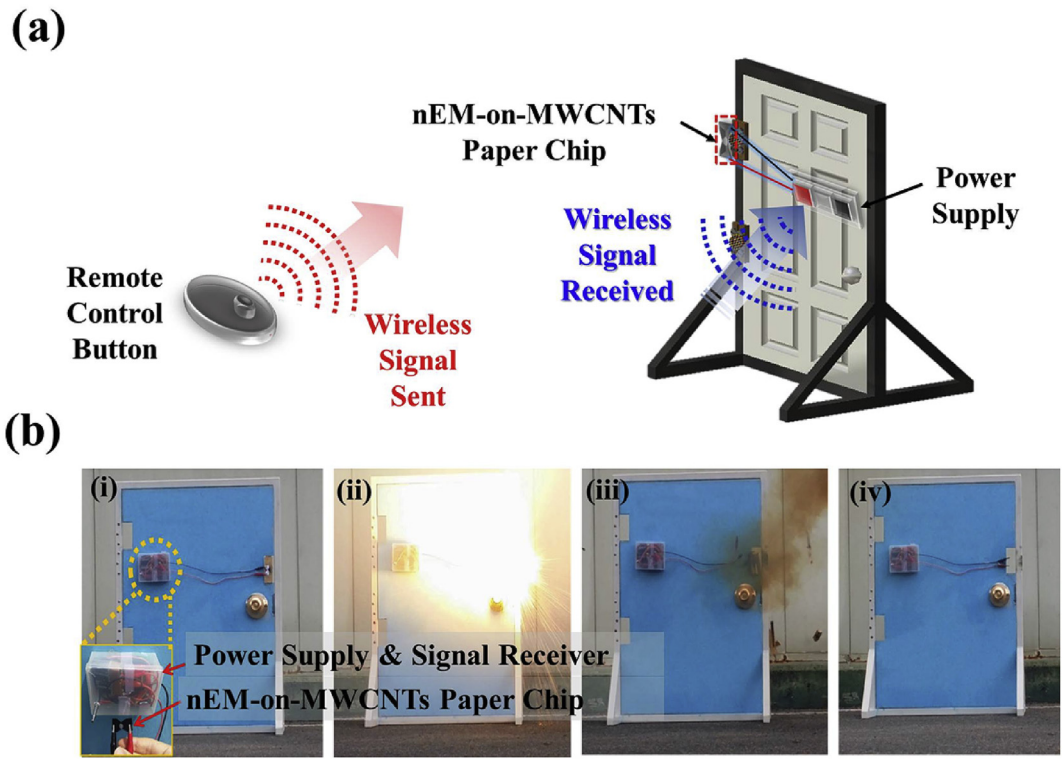

Fig. 5. (a) Schematic and (b) snapshots of the transmission of a wireless signal to initiate explosive door breaching by using the nEM-on-MWCNTs paper chip. The door breaching process consisted of the following four steps: (i) the nEM-on-MWCNTs paper chip was placed on the upper part of the door knob, (ii) it was ignited and subsequently exploded by a remotely transmitted signal, (iii) the door hinge was destroyed by the explosion of the nEM-on-MWCNTs paper chip, and (iv) this completely removed the door hinge, resulting in the opening of the door. (A colour version of this figure can be viewed online.)

MWCNTs paper chip were examined by varying the amount of nEMs; this was accomplished by controlling the thickness of the nEM thin film formed on the paper electrode. The nEM-on-MWCNTs paper chip was ignited in a confined pressure cell tester, as shown in Fig. 4a, by applying a voltage of approximately 15 V. The ignition and explosion responses of the chip were monitored continuously by using a high-speed camera. Fig. 4b shows that the initial ignition and subsequent explosion of the nEM-on-MWCNTs paper chip occurred successfully, owing to the heat generated on the application of a voltage of ~15 V. The combustion characteristics of the nEM-on-MWCNTs paper chip were determined in terms of the ignition delay time, which was ~110 ± 20 ms, the burn rate, which was ~70 ± 10 m/s, and the total burning time, which was ~5.7 ± 0.5 ms. The pressure generated by the ignition of the chip was recorded in situ by using a pressure sensor system installed, as shown in Fig. 4c and d. An nEM thin film with a higher thickness resulted in a higher pressure in a short period. The pressurization rate, which can be defined as the ratio of the maximum pressure to the rise time, was found to increase linearly with an increase in the thickness of the nEM thin film. This suggested that one can readily control the magnitude of the pressure generated as well as the pressurization rate simply by varying the thickness of the nEM thin film used in the nEM-on-MWCNTs paper chip. In this study, the maximum pressure and pressurization rate for Al NP/CuO NP-based thin film with the thickness of 150 μm ignited by MWCNTs-coated paper chip were found to be approximately 5.0 MPa and 0.55 MPa/ms, respectively, as shown in Fig. 4c and d. The same Al NP/CuO NP-based thin film was ignited using tungsten hot-wire for comparison, and its maximum pressure and pressurization rate were found to be approximately 5.7 MPa and 0.57 MPa/ms, respectively, which are very similar with that of nEM-on-MWCNTs paper chip. This suggests that nEM-on-MWCNTs paper chip can be an effective igniter to generate the sufficient explosion reactivity of nEMs.

The nEM-on-MWCNTs paper chip was used for remote explosive door breaching, which is a technique that can be used for evacuation under civil and military emergency situations. To breach the door, the nEM-on-MWCNTs paper chip was connected to a power supply such that it would ignite upon receiving an externally transmitted signal, as shown in Fig. 5a. In this study, the size of nEM-on-MWCNTs paper chip was 1.5 cm in width and 3 cm in length. The thickness of the nEM thin film was ~150 μm was used. The chip was placed on a door hinge and ignited remotely by an electric signal transmitted from a signal input button, which caused a voltage of ~15 V to be applied to the chip. As shown in Fig. 5b, the door hinge was successfully destroyed by remotely igniting and subsequently exploding the nEM-on-MWCNTs paper chip placed on it. This suggested that the nEM-on-MWCNTs paper chips fabricated in this study have potential for use as versatile igniters for both civil and military applications, as they are compact, flexible, portable, stable, and inexpensive.

4. Conclusions

In this work, a MWCNTs-coated paper electrode was fabricated using a vacuum filtration method. With the assistance of peel-off and water washing tests, the adhesion between MWCNTs and paper was found to be strong by van der Waals attraction forces. The electrical resistance was also not appreciably changed by bending it with various curvatures. After applying various applied voltages to the bow-tie-shaped MWCNTs-coated paper electrode, flame was found to suddenly start from its neck area to the electrode at the applied voltages of ~15 V. The MWCNTs-coated paper electrode was then used as a platform to support a nEM thin film, which was

coated on the MWCNTs-coated paper using a spin-coating process. The nEM-on-MWCNTs paper chip was finally assembled, and then it was tested as a compact and flexible igniter connected to a power supply operated by remote signal transmittance system. Finally, the remote ignition and explosion was successfully demonstrated using the nEM-on-MWCNTs paper chip for realizing a door breaching technique, suggesting that such nEM-on-MWCNTs paper chips can be used as compact, flexible, and versatile igniters in various civil and military applications.

Acknowledgment

This research was supported by the Civil & Military Technology Cooperation Program of the National Research Foundation (NRF) of Korea, which is funded by the Ministry of Science, ICT & Future Planning, Korea (No. 2013M3C1A9055407). This research was also partially supported by National Research Foundation of Korea, funded by the Ministry of Science, ICT & Future Planning, Korea (No. 2015R1A2A1A15054036).

Appendix A. Supplementary data

Supplementary data related to this article can be found at http://dx.doi.org/10.1016/j.carbon.2016.12.021.

References

[1] X. Li, X. Liu, J. Huang, Y. Fan, F.Z. Cui, Biomedical investigation of CNT based coatings, Surf. Coatings Technol. 206 (4) (2011) 759–766.
[2] S.F. Oliveira, G. Bisker, N.A. Bakh, S.L. Gibbs, M.P. Landry, M. Strano, S, Protein functionalized carbon nanomaterials for biomedical applications, Carbon 95 (2015) 767–779.
[3] P. Jagtap, S.K. Reddy, D. Sharma, P. Kumar, Tailoring energy absorption capacity of CNT forests through application of electric field, Carbon 95 (2015) 126–136.
[4] W. Wang, Y. Zhu, S. Liao, J. Li, Carbon nanotubes reinforced composites for biomedical applications, BioMed Res. Int. 2014 (2014).
[5] S.K. Vashist, D. Zheng, K. Al-RubeaanLuong, J.H. Sheu, F.S. Sheu, Advances in carbon nanotube based electrochemical sensors for bioanalytical applications, Biotechnol. Adv. 29 (2) (2011) 169–188.
[6] M. Matsuoka, T. Akasaka, Y. Totsuka, F. Watari, Carbon nanotube-coated silicone as a flexible and electrically conductive biomedical material, Mater. Sci. Eng. C 32 (3) (2012) 574–580.
[7] S.G. Prolongo, M. Burón, M.R. Gude, R. Chaos-Morán, M. Campo, A. Urena, Effects of dispersion techniques of carbon nanofibers on the thermo-physical properties of epoxy nanocomposites, Compos. Sci. Technol. 68 (13) (2008) 2722–2730.
[8] N.W.S. Kam, Z. Liu, H. Dai, Functionalization of carbon nanotubes via cleavable disulfide bonds for efficient intracellular delivery of siRNA and potent gene silencing, J. Am. Chem. Soc. 127 (36) (2005) 12492–12493.
[9] I. Firkowska, M. Olek, N. Pazos-Peréz, J. Rojas-Chapana, M. Giersig, Highly ordered MWNT-based matrixes: topography at the nanoscale conceived for tissue engineering, Langmuir 22 (12) (2006) 5427–5434.
[10] S.G. Prolongo, M. Burón, M.R. Gude, R. Chaos-Morán, M. Campo, A. Urena, Effects of dispersion techniques of carbon nanofibers on the thermo-physical properties of epoxy nanocomposites, Compos. Sci. Technol. 68 (13) (2008) 2722–2730.
[11] M. Ono-Ogasawara, T. Myojo, Characteristics of multi-walled carbon nanotubes and background aerosols by carbon analysis; particle size and oxidation temperature, Adv. Powder Technol. 24 (1) (2013) 263–269.
[12] T.C. Lu, J.L. Tsai, Characterizing load transfer efficiency in double-walled carbon nanotubes using multiscale finite element modeling, Compos. Part B Eng. 44 (1) (2013) 394–402.
[13] M. Zhang, S. Fang, A.A. Zakhidov, S.B. Lee, A.E. Aliev, C.D. Williams, R.H. Baughman, Strong, transparent, multifunctional, carbon nanotube sheets, Science 309 (5738) (2005) 1215–1219.
[14] M. Zhang, K.R. Atkinson, R.H. Baughman, Multifunctional carbon nanotube yarns by downsizing an ancient technology, Science 306 (5700) (2004) 1358–1361.
[15] S. Berber, Y.K. Kwon, D. Tománek, Unusually high thermal conductivity of carbon nanotubes, Phys. Rev. Lett. 84 (20) (2000) 4613.
[16] P. Kim, L. Shi, A. Majumdar, P.L. McEuen, Thermal transport measurements of individual multiwalled nanotubes, Phys. Rev. Lett. 87 (21) (2001) 215502.
[17] C. Ge, Y. Li, J.J. Yin, Y. Liu, L. Wang, Y. Zhao, C. Chen, The contributions of metal impurities and tube structure to the toxicity of carbon nanotube materials, NPG Asia Mater. 4 (12) (2012) e32.
[18] C. Choi, J.A. Lee, A.Y. Choi, Y.T. Kim, X. Lepró, M.D. Lima, S.J. Kim, Flexible supercapacitor made of carbon nanotube yarn with internal pores, Adv. Mater. 26 (13) (2014) 2059–2065.
[19] M. Qian, T. Feng, K. Wang, H. Ding, Y. Chen, Q. Li, Z. Sun, Field emission of carbon nanotube films fabricated by vacuum filtration, Phys. E Low-Dimens. Syst. Nanostruct. 43 (1) (2010) 462–465.
[20] W. Xiong, F. Du, Y. Liu, A. Perez Jr., M. Supp, T.S. Ramakrishnan, L. Jiang, 3-D carbon nanotube structures used as high performance catalyst for oxygen reduction reaction, J. Am. Chem. Soc. 132 (45) (2010) 15839–15841.
[21] Y. Tsarfati, V. Strauss, S. Kuhri, E. Krieg, H. Weissman, E. Shimoni, B. Rybtchinski, Dispersing perylene diimide/SWCNT hybrids: structural insights at the molecular level and fabricating advanced materials, J. Am. Chem. Soc. 137 (23) (2015) 7429–7440.
[22] Q.W. Li, Y. Li, X.F. Zhang, S.B. Chikkannanavar, Y.H. Zhao, A.M. Dangelewicz, P.N. Arendt, Structure-dependent electrical properties of carbon nanotube fibers, Adv. Mater. 19 (20) (2007) 3358–3363.
[23] G. Chen, D.N. Futaba, H. Kimura, S. Sakurai, M. Yumura, K. Hata, Absence of an ideal single-walled carbon nanotube forest structure for thermal and electrical conductivities, ACS Nano 7 (11) (2013) 10218–10224.
[24] C. Rossi, A. Estève, P. Vashishta, Nanoscale energetic materials, J. Phys. Chem. Solids 71 (2) (2010) 57–58.
[25] J.Y. Ahn, J.H. Kim, J.M. Kim, D.W. Lee, J.K. Park, D. Lee, S.H. Kim, Combustion characteristics of high-energy Al/CuO composite powders: the role of oxidizer structure and pellet density, Powder Technol. 241 (2013) 67–73.
[26] C. Wu, K. Sullivan, S. Chowdhury, G. Jian, L. Zhou, M.R. Zachariah, Encapsulation of perchlorate salts within metal oxides for application as nano-energetic oxidizers, Adv. Funct. Mater. 22 (1) (2012) 78–85.
[27] M.L. Pantoya, J.J. Granier, Combustion behavior of highly energetic thermites: nano versus micron composites, Propellants, Explos. Pyrotech. 30 (1) (2005) 53–62.
[28] F. Séverac, P. Alphonse, A. Estève, A. Bancaud, C. Rossi, High-energy Al/CuO nanocomposites obtained by DNA-directed assembly, Adv. Funct. Mater. 22 (2) (2012) 323–329.
[29] R. Shende, S. Subramanian, S. Hasan, S. Apperson, R. Thiruvengadathan, K. Gangopadhyay, S. Gangopadhyay, Nanoenergetic composites of CuO nanorods, nanowires, and Al-Nanoparticles, Propellants, Explos. Pyrotech. 33 (2) (2008) 122–130.
[30] S.B. Kim, K.J. Kim, M.H. Cho, J.H. Kim, K.T. Kim, S.H. Kim, Micro- and nanoscale energetic materials as effective heat energy sources for enhanced gas generators, ACS Appl. Mater. Interfaces 8 (2016) 9405–9412.
[31] J.H. Kim, S.B. Kim, M.G. Choi, D.H. Kim, K.T. Kim, H.M. Lee, S.H. Kim, Flash-ignitable nanoenergetic materials with tunable underwater explosion reactivity: the role of sea urchin-like carbon nanotubes, Combust. Flame 162 (4) (2015) 1448–1454.
[32] A. Göçmez, G.A. Yilmaz, F. Peke, S. Özkar, Development of MTV compositions as igniter for HTPB/AP based composite propellants, Propellants, Explos. Pyrotech. 24 (2) (1999) 65–69.
[33] A. Ulas, G.A. Risha, K.K. Kuo, An investigation of the performance of a boron/potassium-nitrate based pyrotechnic igniter, Propellants, Explos. Pyrotech. 31 (4) (2006) 311–317.
[34] R. Rosenberg, L. Berenbaum, Resistance monitoring and effects of non-adhesion during electromigration in aluminum films, Appl. Phys. Lett. 12 (5) (1968) 201–204.
[35] R.E. Hummel, R.T. Dehoff, H.J. Geier, Activation energy for electrotransport in thin aluminum films by resistance measurements, J. Phys. Chem. Solids 37 (1976) 73–80.
[36] J. Li, J.W. Mayer, E.G. Colgan, Oxidation and protection in copper and copper alloy thin films, J. Appl. Phys. 70 (1991) 2820–2827.
[37] R. Ram, M. Rahaman, D. Khastgir, Electrical properties of polyvinylidene fluoride (PVDF)/multi-walled carbon nanotube (MWCNT) semi-transparent composites: modelling of DC conductivity, Compos. Part A Appl. Sci. Manuf. 69 (2015) 30–39.
[38] A. Kamyshny, S. Magdassi, Conductive nanomaterials for printed electronics, Small 10 (17) (2014) 3515–3535.
[39] S. Yao, Y. Zhu, Nanomaterial-enabled stretchable conductors: strategies, materials and devices, Adv. Mater. 27 (9) (2015) 1480–1511.
[40] H.K. Park, S.M. Kim, J.S. Lee, J.H. Park, Y.K. Hong, C.H. Hong, K.K. Kim, Flexible plane heater: graphite and carbon nanotube hybrid nanocomposite, Synth. Met. 203 (2015) 127–134.
[41] J. Lin, H. Zhang, M. Tang, W. Tu, X. Zhang, Improved thermal property of a multilayered graphite nanoplatelets filled silicone resin composite, J. Mater. Eng. Perform. 24 (2) (2015) 920–929.
[42] L.F. Dumée, K. Sears, B. Marmiroli, H. Amenitsch, X. Duan, R. Lamb, D. Buso, C. Huynh, S. Hawkins, S. Kentish, M. Duke, S. Gray, P. Innocenzi, A.J. Hill, P. Falcaro, A high volume and low damage route to hydroxyl functionalization of carbon nanotubes using hard X-ray lithography, Carbon 51 (2013) 430–434.
[43] L. Dumée, K. Sears, J. Schütz, N. Finn, M. Duke, S. Gray, Influence of the sonication temperature on the debundling kinetics of carbon nanotubes in propan-2-ol, Nanomaterials 3 (1) (2013) 70–85.